Selective acylation of chitosan oligomers by several cyclic anhydrides as a 13C NMR quantification method

Paul Morandi, Steve Berthalon, Ghislain David, Aurelien Lebrun, Karine Parra, Claire Negrell

Carbohydrate Polymer Technologies and Applications 7 (2024) 100498

Contents lists available at ScienceDirect

Carbohydrate Polymer Technologies and Applications

journal homepage: www.sciencedirect.com/journal/carbohydrate-polymer-technologies-and-applications

Selective acylation of chitosan oligomers by several cyclic anhydrides as a ^{13}C NMR quantification method

Paul Morandi [a], Steve Berthalon [a], Ghislain David [a], Aurelien Lebrun [b], Karine Parra [b], Claire Negrell [a,*]

[a] ICGM, University Montpellier, CNRS, ENSCM, Montpellier, France
[b] LMP, University Montpellier, CNRS, Montpellier, France

ARTICLE INFO

Keywords:
Chitooligosaccharides (COS)
Glucosamine
Amine protection and deprotection
Acylation
Anhydrides
^{13}C NMR quantification

ABSTRACT

The chemistry of chitosan is a promising way to afford biobased and biodegradable complex materials using highly reactive compounds such as anhydrides. However, the potential applications are limited due to the absence of control over the acylation and the lack of precise characterization. After a model study on glucosamine, a selective acylation method of amines or alcohols of chitosan oligomers using anhydrides has been developed. The N-acylation of chitooligosaccharides has been achieved using several anhydrides and the O-acylation has been achieved in three steps: (1) Amine protection using *p*-anisaldehyde (2) O-acylation (with four anhydrides), and (3) Amine deprotection by removing the protective anisyl groups. Functionalized chitooligosaccharides have been characterized by a precise quantification method using ^{13}C nuclear magnetic resonance spectroscopy. The resulting degrees of substitution show in most of the cases a stochiometric reaction between anhydrides and amines of chitooligosaccharides, and around 70 % of efficiency for O-acylation, proving the promising potential of such modifications. To the best of our knowledge, we describe here the first example of selective acylation of chitooligosaccharides using anhydrides, and most of all the first example of ^{13}C quantitative NMR spectroscopy performed on chitooligosaccharides and its derivatives. These innovative structures are the gateway to the creation of new biosourced and/or biodegradable surfactants.

1. Introduction

Over the years, environmental issues around the world have become more significant, and the production of polymer materials from petroleum derivatives is one of the biggest concerns in this context. The ecological transition being necessary, scientists began to think differently and started looking for any possible application using eco-friendly materials, despite the related constraints. Following this idea, bio-based polymers, such as cellulose, collagen, starch, or chitosan, have been studied in literature (Al-Hazmi et al., 2024; Nasrollahzadeh et al., 2020).

Chitosan is an eco-friendly polymer derived from chitin, the second most abundant natural polymer (after cellulose) that can be found in crustacean shells, insects and fungi (Aranaz et al., 2021; Bhattacharjee et al., 2020; Kou et al., 2022; Mohammad El-Aidie, 2018). Recently, it gained attention by being both bio-based and biodegradable, in addition to its capacity to be chemically modified in various ways (Shrestha et al., 2023). It is a linear polysaccharide composed of two repeating units which are glucosamine (GlcN) and *N*-acetyl-glucosamine (GlcNAc), linked by a glycosidic bond. Its behavior (solubility and reactivity) greatly depends on its molecular weight and degree of acetylation "DA" (ratio of GlcNAc units on all units of the chain) (Aranaz et al., 2021; Bhattacharjee et al., 2020; Kou et al., 2022; Mohammad El-Aidie, 2018). Because of its antimicrobial (Bhattacharjee et al., 2020; Kou et al., 2022; Mohammad El-Aidie, 2018) and antioxidative properties (Aranaz et al., 2021; Mohammad El-Aidie, 2018), chitosan has been investigated for its possible applications in the food industry and agrochemistry (Aranaz et al., 2021; Meyer-Déru et al., 2022; Morin-Crini et al., 2019). Due to their biocompatibility, anti-inflammatory properties (Aranaz et al., 2021) and/or antitumor effects, chitosan and its derivatives have great potential in medicine such as surgery and tissue engineering (Kou et al., 2022), drug delivery (Aranaz et al., 2021) or oncology (Kou et al., 2022). It also has applications in various fields such as cosmetics (Morin-Crini et al., 2019), bitumen (Chapelle et al., 2021a) or water treatment (Holmes et al., 2023; Yang et al., 2016).

* Corresponding author: Postal address: ICGM - UMR5253, Pôle Chimie Balard Recherche, 1919 route de Mende, 34293 Montpellier, France.
E-mail address: claire.negrell@enscm.fr (C. Negrell).

https://doi.org/10.1016/j.carpta.2024.100498

Available online 16 April 2024

The presence of both reactive OH and NH_2 sites on each single unit of chitosan enables various chemical modifications to afford new properties to chitosan and/or allow further chemical modifications for the synthesis of complex materials. Madera-Santana et al. (2018) recently reviewed the different pathways for efficiently grafting chitosan by using carboxylic acid, epoxy, alkene and many other groups. Among them, anhydrides are specifically interesting: first because they can react on both amine and alcohol quantitatively, and secondly because of the choice of anhydrides carrying non-polar chains that can lead to chitosan-based amphiphilic materials.

Few papers introduce some crude chitosan's modifications with cyclic anhydrides such as maleic anhydride (Don & Chen, 2005; Gopal Reddi et al., 2017; Zhang et al., 2007), succinic anhydride (Ranjbar--Mohammadi et al., 2010) or phthalic anhydride (Braz et al., 2020; Ifuku et al., 2011; Ranjbar-Mohammadi et al., 2010) to improve pervaporation, antibacterial or removal properties, or to bring carboxylic functions. The characterization of polysaccharides is still scarce, because of their complex sugar structure, presence of heteroatoms, high viscosity (depending on the molecular weight) and low solubility (Yao et al., 2021). Pure chitosan has already been well studied by Nuclear Magnetic Resonance (NMR) spectroscopy (Mourya et al., 2011; Vårum et al., 1991), but when modified with anhydrides its behavior leads to imprecise analyses. Acylation efficiency was only confirmed by infra-red (FTIR) analyses from which amide function is evidenced by the presence of a characteristic carbonyl peak (Braz et al., 2020; Don & Chen, 2005; Gopal Reddi et al., 2017; Ifuku et al., 2011; Ranjbar-Mohammadi et al., 2010; Zhang et al., 2007). Some ^{13}C NMR analyses of modified chitosan were also performed (Alvarez Echazú et al., 2022; Braz et al., 2020; Don & Chen, 2005) to confirm anhydrides reaction, but most of the spectra lack resolution due to the high molecular weight of used chitosan. Ifuku et al. (2011) reported a quantitative ^1H NMR method of a chemoselective N-phthaloyl chitosan in aqueous media by comparing the isolated proton's peaks of the phthaloyl groups and the proton's peaks of glucosamine ring. This quantitative ^1H NMR method works for phthalic anhydride reaction thanks to the aromatic ring but lacks precision for other anhydrides due to overlapping peaks. In any case, neither FTIR and ^{13}C NMR analyses are able to quantitatively assess the acylation efficiency, and quantitative ^1H NMR analyses are limited to specific anhydrides as aromatic-bearing anhydride (Ifuku et al., 2011). To the authors' knowledge, only two examples of acylation quantification using anhydrides were found in the literature: by elemental analysis (Sousa et al., 2022) and by comparing the product weight before and after acylation (Hasipoglu et al., 2005), but these methods remain very approximate. To date, there is no robust and universal method to characterize and quantify chitosan acylation using anhydrides, both on NH_2 and OH sites.

Recently, chitooligosaccharides (COS) and their derivatives have been studied (Chapelle et al., 2021b) and these have shown an improvement in their properties such as better antimicrobial, anti-tumor, anti-inflammatory and antioxidant activities (Chotphruethipong et al., 2023; Naveed et al., 2019). Thanks to their shorter hydrophilic chain, their functionalization can lead to various structures such as nanomaterials (Nguyen et al., 2019), microgel (Fu et al., 2019), chelating agents (Zhang et al., 2011) or amphiphilic systems (Aranaz et al., 2010; Chapelle et al., 2021c). Unlike native chitosan and due to their low molecular weight, COS is completely soluble in water and in some polar organic solvents, which enables efficient chemical modifications. Furthermore, these COS are less viscous and more soluble in deuterated solvents, thus leading to an easier NMR spectroscopy characterization allowing a quantification of the functionalization. Thus, COS can be used as model compounds to understand the acylation of chitosan using anhydrides.

Here we propose a simple method for selective acylation of COS using various functional anhydrides, in addition to a quantification method. First, a study has been carried out on model molecules to conceive a strategy for selective acylation of glucosamine units. The aims are to subsequently apply this strategy to COS, and then use a precise NMR spectroscopy method to quantify the acylation. As seen in the literature, we expect to modify only amine groups when pure COS are used (Braz et al., 2020; Don & Chen, 2005; Gopal Reddi et al., 2017; Ifuku et al., 2011; Ranjbar-Mohammadi et al., 2010; Zhang et al., 2007). For the same reason, we propose another way to perform selective O-acylation, involving a protection/deprotection method for keeping free amines, based on the primary study on model molecules. For all anhydrides tested, various acylation ratios have been set in order to assess COS reactivity, depending on the targeted site. All modified COS samples have been analyzed by ^1H NMR and 2D ^1H–^{13}C HSQC NMR. Finally, ^{13}C NMR with a helium cryoprobe was used to provide a precise quantification method for modified COS. This work is the first step towards the synthesis of new bio-based compounds having a specific ionic character, which can be tuned by controlling the O/N-acylation as well as the degree of substitution for each acylation. Indeed, according to the pKa of both carboxylic acid and amine groups, 4.8 and 6.5 respectively, the modified oligomers will show either a cationic, a zwitterionic (amphoteric), or an anionic character. The ionic strength of the oligomer will therefore depend on the degree of substitution for both O/N-acylation.

2. Materials and methods

Chitooligosaccharides called COS (M_w: 1400 g.mol^{-1} (DPn = 10) see SI, Fig. S11, Degree of acetylation "DA": 15 %) were obtained from VNF (Hô Chi Minh City, Vietnam). Glucosamine hydrochloride, *p*-anisaldehyde, acetic anhydride (AA), maleic anhydride (MA), succinic anhydride (SA), phthalic anhydride (PA), pyridine and anhydrous sodium acetate were purchased from Sigma Aldrich, and allyl succinic anhydride (ASA) from Gelest. Triethylamine, dichloromethane, ethanol and acetone were purchased from Carlo Erba, methanol from LabKem and diethyl ether from Honeywell. Hydrochloric acid was obtained from Fluka and sodium hydroxide from VWR. Ethyl acetate was obtained from Fisher. Dimethylsulfoxide (DMSO) was purchased from Fluka Chemicals. Finally, deuterated solvents for NMR were purchased from Eurisotop and Innovachem

2.1. Synthesis of 2-(4-Methoxybenzylidene)imino-2-deoxy-D-glucopyranose (1)

1 was synthetized via a NH_2 protection reaction of GlcAm·HCl with *p*-anisaldehyde according to a method described by Cunha et al. (1999). *p*-anisaldehyde (564 μL, 1 eq) was added to a stirred mixture of glucosamine hydrochloride (1.0 g, 1 eq) and 1 N aqueous sodium hydroxide solution (5 ml). Vigorous stirring was maintained for 2 h at room temperature (≈ 25 °C) and the product was collected by filtration, washed with cold water, diethyl ether / ethanol (1:1), and vacuum dried at 60 °C to produce **1** as a white solid (yield = 82 %).

^1H NMR (DMSO-d_6, 400 MHz) δ [ppm] (see SI, **Figure S1**): 8.11 (s, 1H, Hg), 7.68 (d, 2H, Hh, J = 8.7 Hz), 6.98 (d, 2H, Hi, J = 8.7 Hz)), 6.51 (OH), 4.95 (OH), 4.82 (OH), 4.69 (d, 1H, Ha, J = 7.7 Hz), 4.55 (OH), 3.79 (s, 3H, Hj), 3.71–3.49 (d, d, 2H, Hf), 3.42 (t, 1H, Hc, J = 7.0 Hz), 3.22 (t, 1H, He), 3.14 (t, 1H, Hd), 2,79 (t, 1H, Hb, J = 6.7 Hz).

2.2. Synthesis of 2-(4-Methoxybenzylidene)imino-2-deoxy-1,3,4,6-tetra-O-acetyl-D-glucopyranose (2)

2 was prepared by O-acylation of **1** according to a method described by Cunha et al. (1999). First, acetic anhydride (1.59 mL, 10 eq) was added to a stirred dispersion of **1** (0.5 g, 1 eq) in pyridine (2.7 mL, 2 eq) at 0 °C. The resulting mixture was stirred at this temperature until dissolution was complete. It was then kept at room temperature (≈ 25 °C) with stirring for 16 h. The solution was poured into cold water (7 mL) and left in the refrigerator (4 °C) for 1 h. After crystallization, the resulting solid was collected by filtration and washed with cold water,

then recrystallized in ethanol (7 mL) at 60 °C, filtered, washed with cold water again and vacuum dried to afforded **2** (yield = 47 %).

^{1}H NMR ($CDCl_3$, 400 MHz) δ [ppm] (see SI, **Figure S2**): 8.14 (s, 1H, Hg), 7.73 (d, 2H, Hh, J = 8.6 Hz), 6.93 (d, 2H, Hi, J = 8.6 Hz), 6.00 (d, 1H, Ha, J = 8.4 Hz), 5.47 (t, 1H, Hc, J = 9.8 Hz), 5.14 (t, 1H, Hd, J = 9.8 Hz), 4.40–4.11 (m, 2H, Hf, J = 2.12, 4.8 and 12.5 Hz), 3.99 (m, 1H, He, J = 4.5 and 10.2 Hz), 3.85 (s, 3H, Hj), 3.50 (t, 1H, Hb, J = 7.1 Hz), 2.10–1.89 (m, 12H, Hk/Hl/Hm/Hn).

2.3. Synthesis of 2-Amino-2-deoxy-1,3,4,6-tetra-O-acetyl-D-glucopyranosyl hydrochloride (3)

3 was synthetized by a NH_2 deprotection reaction of **2** with HCl according to a method described by Cunha et al. (1999). GlcIm-A-n-$(OAc)_4$ (0.5 g, 1 eq) was dissolved in acetone (8 mL) heated at 60 °C under reflux, and 1 M hydrochloride acid solution (1.07 mL, 1 eq) was added dropwise. Stirring was maintained for 0.5 h and then the solution was cooled to room temperature (≈ 25 °C). Diethyl ether (10 mL) was added to it, and then it was kept in the refrigerator (4 °C) until crystallization. The resulting product was collected by filtration, washed with diethyl ether and vacuum dried at 60 °C to produce **3** (yield = 57 %).

^{1}H NMR (D_2O, 400 MHz) δ [ppm] (see SI, **Figure S4**): 5.98 (d, 1H, Ha, J = 8.8 Hz), 5.50 (t, 1H, Hc, J = 9.4 and 11.4 Hz), 5.16 (t, 1H, Hd, J = 9.4 and 10.8 Hz), 4.42–4.21 (m, 2H, Hf, J = 4.4 Hz), 4.22 (m, 1H, He, J = 2.5 and 10.8 Hz), 3.78 (t, 1H, Hb, J = 8.7 and 11.4 Hz), 2.24–2.12 (m, 12H, Hg/Hh/Hi/Hj).

2.4. Synthesis of 2-(1-Allyl-carboxyethyl)amido-2-deoxy-1,3,4,6-tetra-O-acetyl-D-glucopyranose (4)

4 was synthesized by N-acylation of **3** using allyl succinic anhydride. First, **3** (1 g, 1 eq) was dissolved in ethyl acetate (10 mL) at 0 °C with stirring. Triethylamine (908 μL, 2.5 eq) was added into it and the reaction was maintained for 0.5 h at room temperature (≈ 25 °C). Then ASA (313 μL, 1 eq) was added and the mixture was maintained for 24 h more. The precipitated by-product (Et_3NHCl) was eliminated by filtration, and the filtrate was vacuum dried to obtain the product. It was then dissolved in ethyl acetate (20 mL) and this organic phase was washed with water (3 × 10 mL), HCl 1 M (3 × 10 mL) and water again (3 × 10 mL). Solvent was eliminated by vacuum dried and the resulting solid was washed with diethyl ether, vacuum dried at 60 °C and purified by flash chromatography with dichloromethane / methanol (93/7) to produce **4** (yield = 35 %).

^{1}H NMR ($CDCl_3$, 400 MHz) δ [ppm] (see SI, **Figure S6**): 6.58–6.41 (m, 1H, NH), 5.73 (m, 2H, Hn/Hn'/Ha), 5.35 (m, 1H, Hc), 5.06 (m, 3H, Ho/Ho'/Hp/Hp'/Hd), 4.35 (m, 1H, Hb), 4.25–4.13 (m, 2H, Hf), 3.93 (m, 1H, He), 2.98 (m, 1H, Hl/Hl'), 2.71–2.29 (m, 4H, Hk/Hk'/Hm/Hm'), 2.08–2.03 (m, 12H, Hg/Hh/Hi/Hj).

2.5. Synthesis of 2-(1-Allyl-dicarboximide)−2-deoxy-1,3,4,6-tetra-O-acetyl-D-glucopyranose (5)

5 was prepared by a cyclisation reaction of ASA from **4**. This synthesis was inspired by a method described by Shetgiri and Nayak (2005). **4** (358 mg, 1 eq), acetic anhydride (69.5 μL, 1 eq) and anhydrous sodium acetate (61 mg, 1 eq) were dissolved in acetone (5 mL). The solution was stirred for 24 h at 100 °C under reflux. The precipitated by-product (AcONa) was eliminated by filtration and solvent was evaporated to obtain the desired product. This product was then purified by flash chromatography with dichloromethane / methanol (98/2) to afforded **5** (yield = 55 %).

^{1}H NMR ($CDCl_3$, 400 MHz) δ [ppm] (see SI, **Figure S9**)): 6.45 (d, 1H, Ha), 5.75 (m, 1H, Hc), 5.63 (m, 1H, Hn), 5.10 (m, 3H, Ho/Hp/Hd), 4.31–4.10 (m, 2H, Hf), 4.30 (m, 1H, Hb), 3.94 (m, 1H, He), 2.84 (m, 1H, Hl), 2.73–2.32 (m, 4H, Hk/Hm), 2.09–2.03 (m, 12H, Hg/Hh/Hi/Hj).

2.6. General procedure for the synthesis of N-acylated COS ("COS-N-Anhydride-eq")

All COS-N-Anhydride-eq were synthetized following the same method. A typical experiment for the synthesis of COS-N-SA-0.5 is reported hereafter, the amounts of reagents for the other COS-N-Anhydride-eq syntheses are summarized in SI (see SI,). First, COS (3 g) was dissolved in DMSO (30 mL) at 50 °C with triethylamine (2.12 mL, 1eq/NH_2 of COS, n_{NH2} being calculated following the **Eq. S1,** see SI). Succinic anhydride (761 mg, 0.5 eq/NH_2 of COS) was added to the solution and maintained at 50 °C for 12 h with stirring. The resulting product was precipitated in methanol, collected by filtration, washed with the non-solvent and then vacuum dried at 60 °C to obtain COS-N-SA-0.5 (yield = 30%).

^{1}H NMR (D_2O, 400 MHz) δ [ppm] (see SI, **Figure S15**): 5.12 (Hb'), 4.51 (Hb/Hb''), 4.00–3.30 (Ha'/Ha''/Hc/Hd/He/Hf), 3.08 (Ha), 2.46 (Hh/Hi), 2.00 (Hg).

^{13}C NMR (D_2O, 125 MHz) δ [ppm] (see SI, **Figure S17**)): 178.12 (Cl), 175.37 (Ci), 174.52 (Cg), 97.45 (Cb), 90.50 (Cb'), 78.17–69.60 (Cc/Ce/Cf), 59.89 (Cd), 54.99 (Ca/Ca'), 30.84 (Cj/Ck), 22.00 (Ch)

2.7. Synthesis of COS-Anisyl ("COS-An")

COS-An was synthetized via a NH_2 protection reaction of COS with *p*-anisaldehyde. COS (5 g) was dissolved in 1 N aqueous sodium hydroxide solution (25 mL) and then *p*-anisaldehyde (6.99 g, 2 eq/NH_2 of COS, n_{NH2} being calculated following the **Eq. S1**, see SI) was added to the mixture. Vigorous stirring was maintained for 12 h at room temperature (≈ 25 °C). The product was precipitated in acetone, collected by filtration, washed with cold acetone, ethanol and diethyl ether, and vacuum-dried at 60 °C to afforded COS-An (yield = 60 %).

^{1}H NMR (DMSO-d_6, 400 MHz) δ [ppm] (see SI, **Figure S46**): 8.14 (Hi), 7.69 (Hj), 6.97 (Hk), 4.70 (Ha/Ha'), 3.80 (Hl), 3.49–3.15 (Hb'/Hc/Hc'/Hd/Hd'/He/He'/Hf/Hf'), 2.88 (Hb), 1.81 (Hm).

2.8. General procedure for the synthesis of O-acylated COS-An ("COS-An-O-Anhydride-eq")

All COS-An-O-Anhydride-eq were synthetized following the same method. A typical experiment for the synthesis of COS-An-O-SA-0.5 is reported hereafter, the amounts of reagents for the other COS-An-O-Anhydride-eq syntheses are summarized in SI (see SI, **Table S2**). First, COS-An (1 g) was dissolved in DMSO (10 mL) at 50 °C with triethylamine (519 μL, 1 eq/repeating unit of COS-An, $n_{GlcI/GlcNAc}$ being calculated following the **Eq. S2**, see SI). Succinic anhydride (186 mg, 0.5 eq/repeating unit of COS-An) was added to the solution and maintained at 50 °C for 12 h with stirring. The resulting product was precipitated in acetone, collected by filtration, washed with acetone and then vacuum-dried at 60 °C to obtain COS-An-O-SA-0.5 (yield = 80 %).

^{1}H NMR (DMSO-d_6, 400 MHz) δ [ppm] (see SI, **Figure S50**): 8.14 (Hi), 7.68 (Hj), 6.98 (Hk), 4.70 (Ha/Ha'), 3.80 (Hl), 3.49–3.15 (Hb'/Hc/Hc'/Hd/Hd'/He/He'/Hf/Hf'), 2.88 (Ha), 2.30 (Hm/Hn), 1.78 (Hh)

2.9. General procedure for the synthesis of O-aceylated COS ("COS-O-Anhydride-eq")

All COS-O-Anhydride-eq were synthetized by the removal of anisyl group in the corresponding COS-An-O-Anhydride-eq, following the same method. A typical experiment for the synthesis of COS-O-SA-0.5 is reported hereafter, the amounts of reagents for the other COS-O-Anhydride-eq syntheses are summarized in SI (see SI, **Table S3**). First, COS-An-O-SA-0.5 (1 g) was dissolved in H_2O (20 mL) at 50 °C, then 12 M aqueous HCl (225 μl, 1eq/Anisyl of COS-An-O-SA-0.5, n_{anisyl} being calculated following the **Eq. S3**, see SI) was added dropwise and the solution was stirring 2 h at 50 °C. The crude product was obtained by diluting the reaction media in MeOH, and all the solvents were removed

under vacuum. The final product was then obtained by solubilization in DMSO, precipitation in dichloromethane (DCM), collected by filtration, washed with DCM and finally dried under vacuum at 60 °C to afforded COS-O-SA-0.5 (yield = 30%).

^{1}H NMR ($D_2$0, 500 MHz) δ [ppm] (see SI, **Figure S77**): 5.5–5.2 (Hg/Hg'), 4.6–4.4 (Hb/Hb'/Hf'), 4.4–3.4 (Ha'/Hc/Hd/Hd'/He/Hf), 3.21 (Ha), 2.8–2.5 (Hi/Hj), 2.1 (Hh)

^{13}C NMR (D_2O, 125 MHz) δ [ppm] (see SI, **Figure S78**): 178–174 (Ch/Cj/Cm), 101.20 (Cb'), 97.46 (Cb), 91–88 (Cg/Cg'), 80–67 (Cc/Ce/Cf/Cf'), 62.76 (Cd'), 60 (Cd), 55.79 (Ca), 54 (Ca'), 31–29 (Ck/Cl), 22.15 (Ci)

2.10. NMR characterization of model molecules (from 1 to 5), "COS-An" and "COS-An-O-Anhydride-eq"

^{1}H and 2D NMR spectra were recorded at 298 K on both Bruker Avance III 500 MHz NMR spectrometer using TCI Cryoprobe Prodigy® or Bruker Avance III HD 400 MHz spectrometer equipped with BBI probe. Chemical shift data are given in δ ppm calibrated with residual protic solvent (e.g. D_2O: 4.79 ppm $-^{1}$H). In addition, 2D homonuclear ^{1}H–^{1}H g-COSY (2 scans, 512 real (t1) × 2048 (t2) complex data points) and 2D heteronuclear spectra ^{13}C-^{1}H g-edited HSQC (8–96 scans, 128–512 real (t1) × 2048 (t2) complex data points) were acquired to assign the compound (16 scans, 512 real (t1) × 2048 (t2) complex data points). Spectra were processed and visualized with Topspin 3.6.2 (Bruker Biospin) on a Linux station.

2.11. ^{1}H and 2D NMR characterization of "COS-N-Anhydride-eq" and "COS-O-Anhydride-eq"

^{1}H and 2D NMR spectra were recorded at 298 K on a Bruker AVANCE III 500 NMR spectrometer operating at 500.17 MHz equipped with a 5 mm ^{1}H/X BBO cryoprobe Helium. All the data were processed with Bruker Topspin 3.6.2 software. The pulse sequence used is a sequence with decoupling during acquisition, multiplicity editing during selection step and phase sensitive using echo/antiecho. For 2D ^{1}H/^{13}C-spectra, the spectral widths are 5000 Hz and 20,833 Hz in ^{1}H and ^{13}C dimensions, respectively. The experiments were acquired using 16 steady state scans, 32 transients and data matrix size of 2048 (0.21 s acquisition time).

2.12. Quantitative ^{13}C NMR characterization of "COS-N-Anhydride-eq" and "COS-O-Anhydride-eq"

^{13}C NMR spectra were recorded at 298 K on a Bruker AVANCE III 500 NMR spectrometer operating at 500.17 MHz equipped with a 5 mm ^{1}H/X BBO cryoprobe Helium. All the data were processed with Bruker Topspin 3.6.2 software. The pulse sequence used is a sequence with inverse gated decoupling. Chromium(III) acetyl acetonate $Cr(acac)_3$ was used as a relaxation agent leading to a relaxation delay of 10 s and 4096 scans.

3. Results and discussion

3.1. Model synthesis

The chemical modification of chitosan is always a challenge. Its polysaccharide nature leads to obvious synthesis constraints such as low solvent solubility, low reactivity or multiple reaction sites (in the case of reaction with anhydride). Assessing the modification efficiency can also be hard to achieve, once more due to its polysaccharide nature. For those reasons, a model synthesis has been made using glucosamine hydrochloride (GlcAm·HCl), which represents a major part of chitosan repeating units (Scheme 1).

The purpose of this model synthesis was to develop a strategy for selective acylation for subsequently applying it to COS. The obtained products will help us to assess the characterization of anhydride-modified COS. This synthesis is based on the work of Cunha et al. (1999), and is suitable to our goal for multiple reasons, such as the first protection step made in aqueous conditions, or the second step involving an anhydride (which can be further adapted with multiple anhydrides onto COS).

The amine protection/deprotection process involves the use of *p*-anisaldehyde, which is a real contribution when applying this process to COS. Indeed, the chemical shift of the aromatic ring of *p*-anisaldehyde in a ^{1}H NMR spectrum can be easily isolated and used to prove the amine full protection (see SI, **Figure S1**). By comparing the integrations of the signal corresponding to the imine proton (HC—N=C<u>H</u>) and the signal corresponding to the glucosamine ring proton in the α-position of the nitrogen (<u>H</u>C—N=CH), the degree of protection can be calculated. In this case, both integrations have the same value, meaning that no unprotected amines are left. In addition, 2D ^{1}H–^{13}C HSQC NMR analyses have been carried out to observe the shift of the glucosamine ring proton

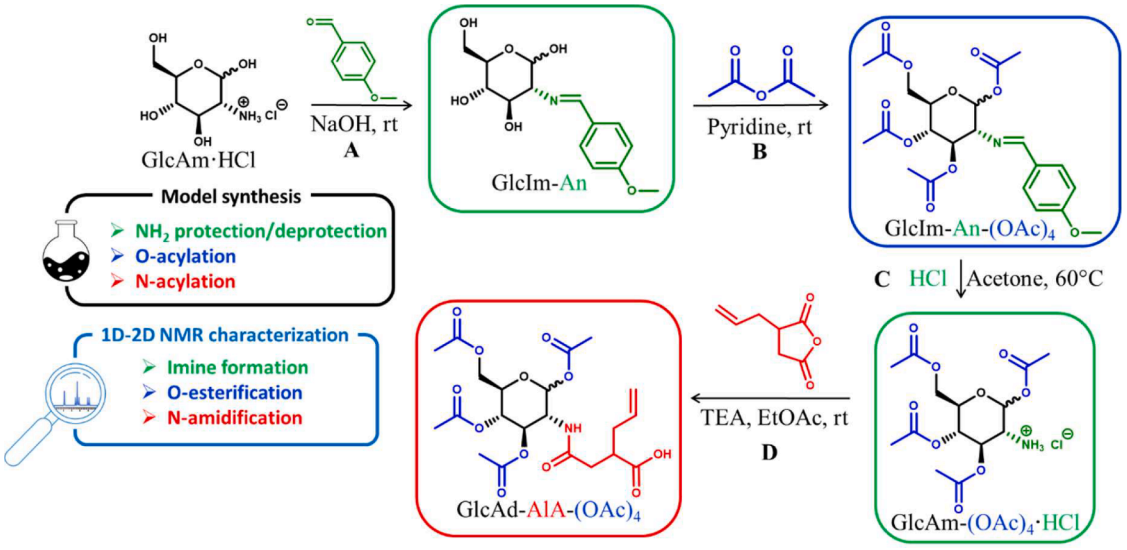

Scheme 1. Synthetic pathway for selective acylation model reaction onto glucosamine in four steps: A. Amine protection using *p*-anisaldehyde; B. O-acylation using acetic anhydride; C. Imine group removal and amine regeneration using hydrochloric acid; D. N-acylation using allyl succinic anhydride.

and carbon in the α-position of the nitrogen (*Fig. 1*). Although the proton does not have a significant shift (from 3.1 to 2.8 ppm), the carbon shifted from 57 ppm to 78 ppm, which will be a good marker of the protection when applying this process on COS.

As seen in *Fig. 1*, glucosamine hydrochloride has an α and a β anomers, and *p*-anisaldehyde will selectively react on the β-anomer, due to the configuration which makes the NH_2 group more available than in the α-anomer because of the steric hindrance. In fact, the α-anomer of 1 is also present in the purified product, but in a much lower proportion compared to the β-anomer of **1**, explaining why it cannot be seen properly in the $^{1}H–^{13}C$ HSQC spectrum (*Fig. 1*). In our case, this is relevant because the glucosamine units in COS are actually in the β configuration, which allows us to not consider the α-anomer of glucosamine for the rest of the model synthesis.

The protection of hydroxyl groups using acetic anhydride is the model synthesis second step. Once more, this step is perfectly adapted to our goal: O-acylation of COS is possible without affecting any amine (because of the imine protection), in addition to protecting the hydroxyl group for further N-acylation in the case of the model synthesis. Indeed, hydroxyl protection is not necessary for N-acylation on COS due to the higher reactivity of amine groups (as seen in the literature (Braz et al., 2020; Don & Chen, 2005; Gopal Reddi et al., 2017; Ifuku et al., 2011; Ranjbar-Mohammadi et al., 2010; Zhang et al., 2007)), but it is probably required in the case of the model synthesis. Glucosamine hydrochloride bears 4 different hydroxyl groups (whereas repeating units of chitosan have only 2 hydroxyl functions) and doesn't have as much steric hindrance as on the chitosan polymer chain. Considering this, the full protection of the hydroxyl groups is mandatory to be sure that the acylation will be fully targeted on the nitrogen without any unwanted side reactions, in order to properly characterize the final product (**2**).

As seen in the ^{1}H NMR spectrum of the obtained **2** (see SI, **Figure S2**), anhydride has efficiently reacted on all hydroxyl groups of **1**, without affecting the N-protective group. The $^{1}H–^{13}C$ HSQC spectrum also confirms that the anisyl group is not affected by the O-acylation, as the carbon chemical shift of the imine is still around 70 ppm (see SI, **Figure S3**)

The third step in the model synthesis involves the removal of the anisyl group leading to amine regeneration. This protection/deprotection process involving *p*-anisaldehyde is particularly interesting for this work, owing to the deprotection step. Indeed, a typical amine protection using $(Boc)_2O$ (Di-tert-butyl dicarbonate) could have been used, but the deprotection process involves the use of TFA (Trifluoroacetic acid) in excess, which is a strong acid. In these conditions, the O-acylation may be affected by the TFA during the deprotection process. In our conditions, the anisyl group removal using a stoichiometric amount of hydrochloric acid allows us to completely regenerate the amine without affecting the O-acylation (see SI, **Figure S4**). As the chemical shift of the glucosamine ring proton in α-position of the nitrogen is barely the same before and after anisyl removal (respectively HC—N═CH and HC—NH_2·HCl, both around 3.5 ppm), a $^{1}H–^{13}C$ HSQC NMR analysis has been made to confirm the carbon shift (HC—N═CH having a signal around 70 ppm and HC—NH_2·HCl around 55 ppm), proving the full regeneration of amine (see SI, **Figure S5**).

Finally, the last step of the model reaction is focused on the N-acylation. As the model synthesis aimed to help the characterization for further COS modifications, allyl succinic anhydride has been chosen instead of acetic anhydride, to avoid any NMR spectrum overlapping. Allyl succinic anhydride is not symmetrical, this reaction results in an isomer mixture of **4**, depending on the anhydride cycle opening (see SI, **Figure S6**). To confirm this, a high-temperature dehydration reaction has been carried out in order to obtain a succinimide cycle, thus avoiding the isomer mixture. ^{1}H NMR spectrum of the product **5** confirms this assumption (see SI, **Figure S9**).

Yet, the NMR analyses of compound **4** confirm the full reaction of allyl succinic anhydride onto amine (Fig. 2, and see SI, **Figure S6, Figure S7** and **Figure S8**). This last step allows us to use the ^{13}C NMR spectrum of **4** (Fig. 2) as a reference for the ^{13}C NMR spectrum of acylated COS assignment, hence allowing acylation quantification.

When applying COS acylation using anhydrides, the signal of the glucosamine ring carbon in the α-position of the primary alcohol can be used as a reference peak. Indeed, even though the proton signal will shift in ^{1}H NMR before and after the anhydride reaction, the carbon won't shift a lot and will stay around 60 ppm (see respectively Fig. 1 and SI **Figure S5**). By calibrating the integration on this last carbon peak, the acylation efficiency can be easily determined using the carbon signals of the reacted anhydride. Taking the example of the allyl succinic anhydride as used in the model reaction, the carbons of the vinyl group are well isolated and can be an efficient marker (*Fig. 2*).

Each anhydride used in this work has its own isolated peaks on the ^{13}C NMR spectrum that can be used to assess the acylation. It can be noticed that all anhydrides have carbonyl groups that can potentially be used, but there is a risk of overlapping with the carbonyl of N-acetyl-

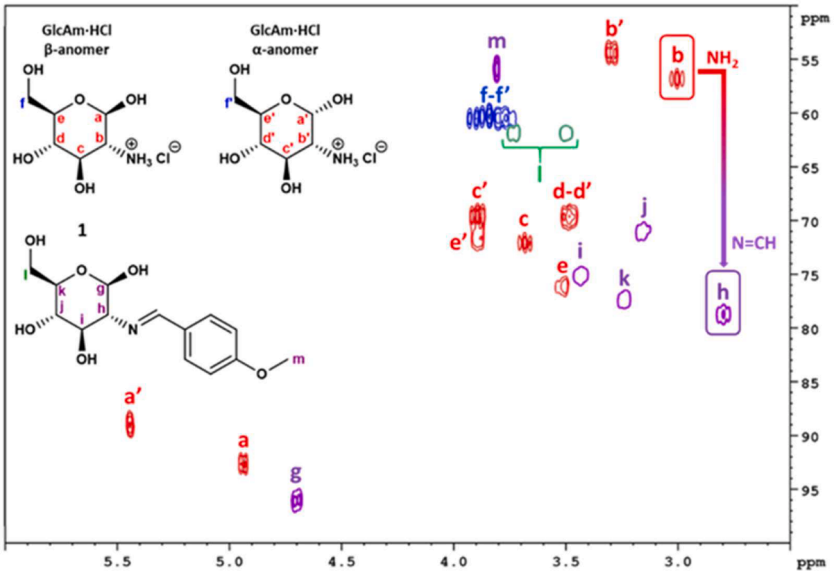

Fig. 1. Overlay of $^{1}H–^{13}C$ HSQC NMR spectrum (400 MHz) and assignment of GlcAm·HCl in D_2O (CH/CH_3 in red and CH_2 in blue) and the molecule 1 in DMSO-d_6 (CH/CH_3 in purple and CH_2 in green).

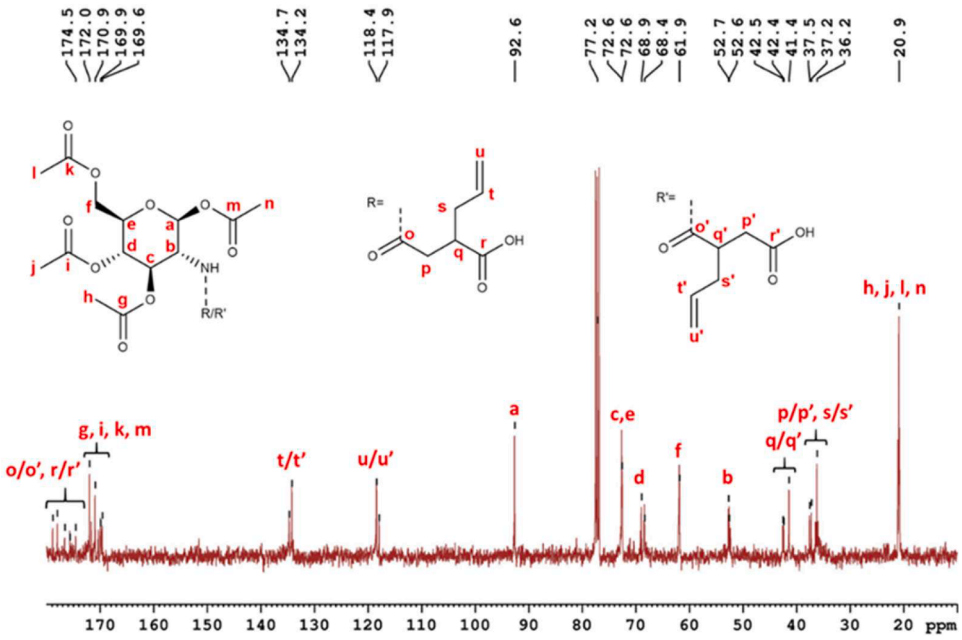

Fig. 2. ^{13}C NMR spectrum (100 MHz, $CDCl_3$) and carbon assignment of 4.

glucosamine (GlcNAc) units present in chitosan.

3.2. Preparation and characterization of N-acylated-COS

According to the literature (Braz et al., 2020; Don & Chen, 2005; Gopal Reddi et al., 2017; Ifuku et al., 2011; Ranjbar-Mohammadi et al., 2010; Zhang et al., 2007), the reaction of anhydrides onto unmodified COS will directly lead to amine groups acylation. Four different anhydrides have been used with pure COS, with anhydride/NH_2 molar ratio of 0.2, 0.5 and 1, allowing us to evaluate the reactivity of the N-acylation (see step **A** from Scheme 2). As the anhydride molar ratio is dependent on the amine groups of COS, the degree of acetylation (DA) has been determined by quantitative ^{13}C NMR spectroscopy, using the same method that will be used to assess acylation efficiency. The resulting spectrum (see SI, **Figure S10**) indicates a DA close to 15 %.

First and foremost, we used succinic anhydride *"SA"* because its simple structure makes the NMR spectra interpretation easier. Indeed, the two CH_2 groups of SA in the α-position of the carbonyl can be spotted in both ^1H NMR and ^{13}C NMR. Therefore, before using ^{13}C NMR to precisely quantify the acylation, ^1H NMR spectra can be used to check if the reaction took place (see SI, **Figure S12**). The signal of the CH_2 in the α-position of the carbonyl at 2.5 ppm proves the opening of the succinic anhydride cycle (whereas in pure succinic anhydride, these signals are around 2.9 ppm). In addition, the peak integration of the CH in the α-position of the amines at 3.1 ppm clearly decreases from 1 to 0.8 (calibrate using the acetyl peak at 2 ppm).

^1H–^{13}C HSQC NMR analyses allowed assessing that the acylation was exclusively performed onto amine groups. By comparing the HSQC spectra of COS-N-SA-0.2, COS-N-SA-0.5 and COS-N-SA-1 (see SI, respectively **Figure S13, Figure S16** and **Figure S19**), the increasing spots of CH in α-position of amide groups are clearly seen, and there are no signs of shifting concerning the CH_2 in α-position of alcohols. Nevertheless, a slight shift of CH_2 in the α-position of alcohols can be spotted in the carbon spectrum of COS-N-SA-1 (see SI, **Figure S20**), proving that the anhydride will also react onto alcohols after all amines have reacted. To confirm this hypothesis, acylation using succinic anhydride has been made with 1.5 equivalent compared to amine groups. The HSQC spectrum of the obtained product confirmed our expectation (see SI, **Figure S21**), as the proton signals of the CH_2 in α-position of primary alcohol are clearly shifting from 3.4 to 3.8 to 4–4.5 ppm, while

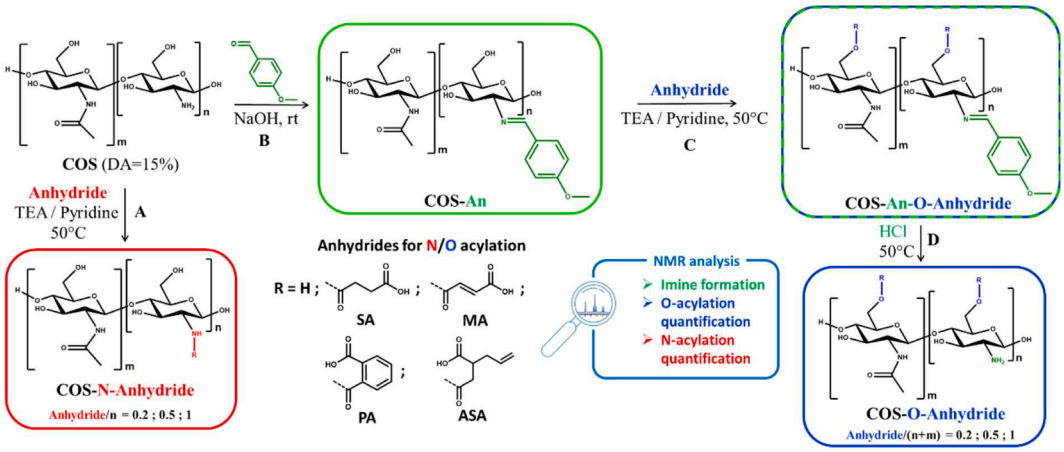

Scheme 2. Synthetic pathway for N-acylation (1 step-red way) or O-acylation (3 steps-green/blue way) of COS: A. N-Acylation of COS; B. Amine protection using *p*-anisaldehyde onto COS; C. O-acylation of COS-An; D. Regeneration of amines in COS-An-O-Anhydride.

all the amines are converted to amides.

However, due to the width of the peaks and their overlapping, quantifying the acylation using the ^{1}H NMR spectrum is very approximate and lacks precision. According to the HSQC spectra of succinic anhydride modified COS (see SI, respectively **Figure S13, Figure S16** and **Figure S19**), in correlation with the observations of the model synthesis, quantitative ^{13}C NMR spectroscopy is a way more precise and can assess acylation efficiency.

Indeed, the carbon spectra are simpler than the corresponding proton spectra since they suffer from much fewer signal overlaps and have a better resolution. The aim was to obtain a spectrum displaying all the carbon resonances of the compound under investigation with a sufficient signal to noise (using a cryoprobe) and in a reasonable amount of time (adding a small amount of chromium(III) acetylacetonate).

Specific signals have then been selected purposely to calibrate all the integrations, which will directly lead to a proper acylation quantification (*Fig. 3*).

The carbon in the α-position of primary alcohol (60 ppm) is present on both glucosamine (GlcN) and N-acetyl-glucosamine (GlcNAc) units, meaning that they can be all integrated and used as a reference for the COS backbone (with a value of 1). Then, the integration of the two CH_2 for the anhydride (spotted at 31–34 ppm) leads to a precise quantification of the acylation calculated thanks to the following equation (Eq. (1)):

$$NH_2\ DS_{COS-N-SA}(\%) = \left(\frac{\int (Cj/Ck)/2}{\int Cd * [1 - DA]}\right) * 100 \qquad (1)$$

Eq. (1) is the ratio between the number of reacted anhydride group and the backbone of the COS, more specifically the glucosamine units which represent the major part of the COS backbone. The value of "$\int (Cj/Ck)$" is divided by 2 because the integration considers the two carbons of the succinic anhydride. As said previously, the carbons in the α-position of primary alcohol represent the whole COS chain, therefore the value of "$\int Cd$" is used as the reference and is set to 1. Finally, "[1-DA]" is added to consider only glucosamine units of the backbone, because N-acetyl-glucosamine units are not affected by the anhydride. In our case, the degree of acetylation "DA" is equal to 15 %. For all anhydrides, the equation for the degree of substitution is nearly the same, just adapted to the carbon used for the quantification. Only COS modified with 1 equivalent of phthalic anhydride (COS-N-PA-1) could not have been characterized, due to lack of solubility in the deuterated solvents. All the ^{1}H, HSQC and quantitative ^{13}C NMR spectra of all N-acylated COS are given in supporting information (see SI, from **Figure S12** to **Figure S45**). All the resulting degrees of substitution are gathered in Table 1.

The experimental degrees of substitution concerning the N-acylated COS show stoichiometric reactions for all the anhydrides using triethylamine as a catalyst. For maleic anhydride "MA" reactions, pyridine was used as a catalyst. Triethylamine was indeed not efficient, probably because maleic anhydride and triethylamine can form a complex in basic conditions, as already reported in the literature (Mayahi & El-Bermani, 1973). Nevertheless, the lower basicity of pyridine may explain the discrepancy between experimental and theoretical DS values. For the other anhydrides, the experimental DS is very close to the theoretical one, even slightly higher in some cases (52 % of amines in "COS-N-ASA-0.5″ are acylated instead of the expected maximum value of 50 %). The main reason explaining this observation is related to the DA determination (determined using quantitative ^{13}C NMR, see **Figure S10**). The N-acylation affecting only the glucosamine units of COS, the amount of anhydride used is directly related to the ratio of glucosamine units compared to the whole chain, i.e. "(1-DA)" (known as the degree of deacetylation "DD"). There is in fact a margin of error (around 5 %) from NMR explaining the slightly higher anhydride equivalent compared to amines. For the same reason and as explained before, a low reaction onto alcohols occurs when all the amines have reacted with anhydrides (in the case of "COS-N-SA-1" and "COS--N-ASA-1", see SI respectively **Figure S20** and **Figure S45**). In these specific cases, the degree of substitution for alcohols is calculated thanks to the following equation (Eq. (2)):

$$OH *\ DS_{COS-N-SA-1}(\%) = \left(\frac{\left[\int (Cj/Ck)/2\right] - [1 - DA]}{\int (Cd/Cd)}\right) * 100 \qquad (2)$$

Finally, it should be noticed that unlike succinic and allyl succinic anhydride ("SA" and "ASA"), the use of phthalic anhydride ("PA") is slightly less efficient for the same reaction conditions. Indeed, the lower degree of substitution and the traces of unreacted phthalic anhydride in the NMR spectra (see SI, **Figure S33** and **Figure S36**) confirm that phthalic anhydride did not totally react. The presence of the aromatic ring induces steric hindrance that may explain this lower reactivity.

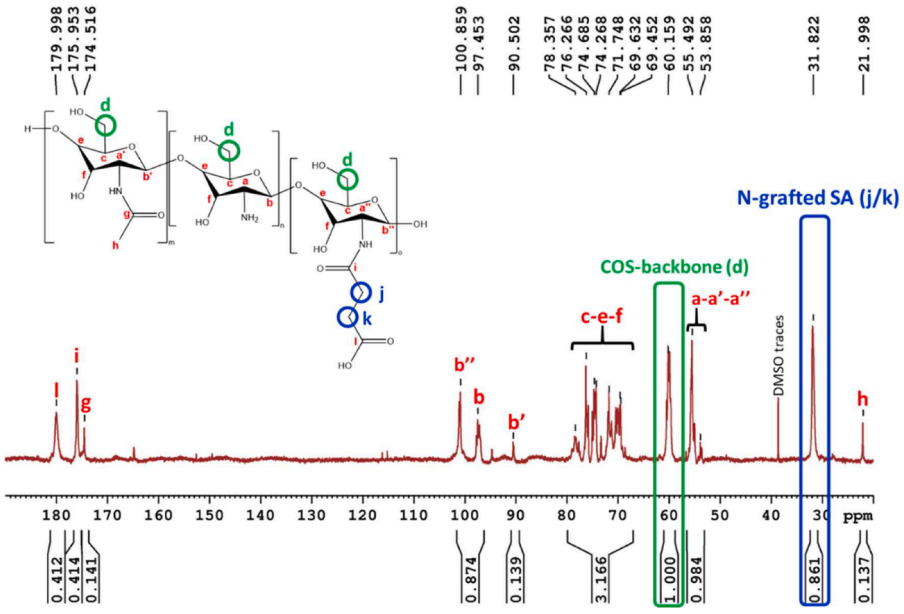

Fig. 3. ^{13}C NMR spectrum (D_2O, 125 MHz) of COS-N-SA-0.5 with the preferred signals for assessing the acylation.

Table 1
Summary of all acylated COS.

Used anhydride [a]	Carbon used for assessing experimental DS [b]	Theoretical DS (%) [c]	Experimental NH_2 DS (%) [d]	Experimental OH DS (%) [e]	COS reference [f]
"SA" 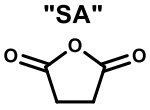	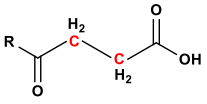	20	21 ± 1	0	COS-N-SA-0.2
			/ [g]	15 ± 0.8	COS-O-SA-0.2
		50	51 ± 2.5	0	COS-N-SA-0.5
			/ [g]	39 ± 2	COS-O-SA-0.5
		100	100 ± 5	4 ± 0.2	COS-N-SA-1
			/ [g]	75 ± 3.8	COS-O-SA-1
"MA" 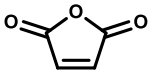	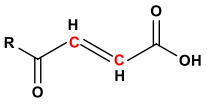	20	16 ± 0.8	0	COS-N-MA-0.2
			/ [g]	10 ± 0.5	COS-O-MA-0.2
		50	39 ± 2	0	COS-N-MA-0.5
			/ [g]	26 ± 1.3	COS-O-MA-0.5
		100	67 ± 3.4	0	COS-N-MA-1
			/ [g]	40 ± 2	COS-O-MA-1
"PA" 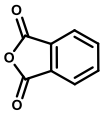	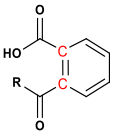	20	17 ± 0.9	0	COS-N-PA-0.2
			/ [g]	15 ± 0.8	COS-O-PA-0.2
		50	43 ± 2.1	0	COS-N-PA-0.5
			/ [g]	37 ± 1.9	COS-O-PA-0.5
"ASA" 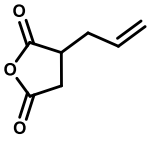	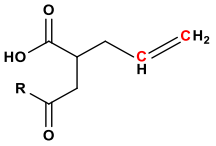	20	21 ± 1	0	COS-N-ASA-0.2
			/ [g]	16.5 ± 0.8	COS-O-ASA-0.2
		50	52 ± 2.6	0	COS-N-ASA-0.5
			/ [g]	31 ± 1.5	COS-O-ASA-0.5
		100	100 ± 5	4 ± 0.2	COS-N-ASA-1
			/ [g]	70 ± 3.5	COS-O-ASA-1

[a] structure of the anhydride used for acylation and the corresponding abbreviation ("SA" for succinic anhydride, "MA" for maleic anhydride, "PA" for phthalic anhydride, "ASA" for allyl succinic anhydride)
[b] Carbon used in the corresponding ^{13}C NMR spectrum for acylation quantification
[c] Determined depending on the equivalent of anhydride used for the N and O acylation of COS
[d] Calculated using selected carbon in the corresponding ^{13}C NMR spectrum, with a margin of error of 5%
[e] Calculated using selected carbon in the corresponding ^{13}C NMR spectrum, with a margin of error of 5%
[f] Name of the corresponding acylated COS. All the ^{13}C NMR spectra used for assessing the acylation are given in the SI
[g] Protected amine.

3.3. Preparation and characterization of O-acylated-COS

Due to the higher reactivity of amine compared to alcohol, the reaction of anhydride with pure COS did not affect hydroxyl groups, as long as free amine groups were available. Then, the protection of amine groups is mandatory for O-acylation of COS. Therefore, the O-acylated COS have been synthesized in 3 steps according to the previously described model reaction (see steps **B, C** and **D** from Scheme 2): protection of amine groups of COS using *p*-anisaldehyde, leading to COS-anisyl named "COS-An"; O-acylation using different anhydrides (with various DS) of COS-An, leading to COS-anisyl-O-anhydride-equivalent named "COS-O-An-Anhydride-eq"; regeneration of free amine groups by removal of anisyl group in COS-An-O-Anhydride-eq, leading to the final product COS-O-anhydride-equivalent named "COS-O-Anhydride-eq".

The amine protection process of COS is directly adapted from the model reaction (see step **B** in Scheme 2). COS being less reactive than glucosamine hydrochloride, the molar ratio of *p*-anisaldehyde/NH_2 has been raised to 2 (compared to 1 for the model reaction), in addition to a longer reaction time, thus affording the highest degree of protection as possible. As observed from ^1H NMR spectrum of product **1** obtained from the model reaction (see SI, **Figure S1**), the chemical shift of the grafted anisyl group is isolated from the other glucosamine ring signals, allowing us to check whether the amine is protected. Indeed, the ^1H NMR spectrum of the obtained COS-An confirms that amine protection occurred, mostly proved by the presence of the imine proton (HC—N═CH) at 8.14 ppm (see SI, **Figure S46**). Nevertheless, the signals of the glucosamine ring proton in the α-position of both amine and imine are overlapping and cannot be distinguished from ^1H NMR spectroscopy. On the other hand, the associated carbon is clearly shifting from 55 ppm (HC—NH_2) to 75 ppm (HC—N═C), therefore ^1H–^{13}C HSQC analysis has been performed on COS-An to properly spot any residual amine groups. The resulting 2D spectrum (see SI, **Figure S47**) does not show any traces of unprotected amine groups, and the carbon associated with the proton signal at 3 ppm is clearly attached to an imine group (75 ppm), proving the full protection of the amine. The resulting COS-An has then been used for O-acylation.

The O-acylation of COS-An has been done using the same method as for the N-acylation (see step **C** in Scheme 2). The same four anhydrides have been used, varying the anhydride/OH ratios. O-acylated COS have to be soluble in D_2O to perform ^{13}C NMR, which led to limited DS in the case of non-polar anhydride reaction onto COS (such as phthalic anhydride "PA" and maleic anhydride "MA"). For this reason and knowing that there are two hydroxyl groups per repeating unit of COS, the anhydride/OH molar ratios used for the acylation have been set to 0.1, 0.25 and 0.5. However, for better comprehension, the different anhydride equivalents (and the experimental degrees of substitution) will be described compared to the repeating units of COS (both GlcN and GlcNAc), leading to anhydride/(GlcN-GlcNAc) molar ratios equal to 0.2, 0.5 and 1. By setting these molar ratios, the maximum number of reacted anhydrides onto alcohols is nearly the same as the number of reacted anhydrides onto amines of COS when using anhydride/NH_2 molar ratios of 0.2, 0.5 and 1.

After the O-acylation of COS-An, the resulting products have been analyzed by both ^1H and ^1H–^{13}C HSQC NMR spectroscopy. The following discussion is based on the results concerning the O-acylation using 0.5 equivalents of succinic anhydride (COS-An-O-SA-0.5), and subsequently its deprotection (COS-O-SA-0.5). Although the ^{13}C quantification couldn't have been done on these products (the quantification method was revealed to be unsuccessful in DMSO-d_6), the anhydride reaction onto COS-An was confirmed by the presence of the reacted anhydride in the ^1H NMR spectrum (see SI, **Figure S50**). Moreover, the

^{1}H–^{13}C HSQC spectrum does not show any alteration of the protective group, as the anisyl group is still present around 7–8 ppm and the proton at 3 ppm is attached to the carbon at 75 ppm (see SI, **Figure S51**), confirming the selective acylation of alcohols of COS-An. All the ^{1}H and ^{1}H–^{13}C HSQC NMR spectra of all O-acylated COS-An are given in supporting information (see SI, from **Figure S48** to **Figure S71**)

The final O-acylated COS has then been obtained by removing the protecting group of the corresponding O-acylated COS-An, regenerating the amine groups of COS. This final step is adapted from the model synthesis (see step **D** in Scheme 2). Chlorohydric acid is used to remove the anisyl group, therefore the experimental conditions have been studied and carefully chosen to avoid any hydrolysis of the reacted anhydride. Indeed, the first test of deprotection has been done using a slight excess of HCl compared to anisyl group (molar ratio HCl/Anisyl was around 1.2), in addition to a high reagent concentration (1 g of O-acylated COS-An in 10 mL of H_2O). Although the deprotection worked, the analysis of the resulting product clearly shows an alteration of the previously used anhydride, proved by the presence of molecular succinic acid at 2.4 ppm (see SI, **Figure S72** and **Figure S73**). By adding a stochiometric amount of HCl (molar ratio HCl/Anisyl at 1), and performing the deprotection in diluted conditions (1 g of O-acylated COS-An in 20–30 mL of H_2O), the anisyl group was totally removed without affecting the previous O-acylation (see SI, **Figure S77** and **Figure S78**). The final product was soluble in D_2O, allowing us to assess the O-acylation using quantitative ^{13}C NMR spectroscopy (Fig. 4).

The O-acylation has been determined using the same methodology as the N-acylation: the carbon in α-position of the primary alcohol and the corresponding ester ($\underline{C}H_2$–OH and $\underline{C}H_2$–O-R at 60–62 ppm) were used as a reference to represent the COS backbone (with a value of 1), and the value of the used anhydride is measured from Fig. 4, the two $\underline{C}H_2$ of the succinic anhydride were used. The degree of substitution is finally calculated thanks to the following equation (Eq. (3)):

$$OH\ DS_{COS-O-SA}(\%) = \left(\frac{\int Ck/Cl)/2}{\int (Cd/Cd')}\right) * 100 \quad (3)$$

Eq. (3) is similar to Eq. (1) (for the N-acylation), as it is a ratio between the number of acylated units and the COS backbone. It should be noticed that unlike Eq. (1), the degree of acetylation "DA" is not considered here because the O-acylation can occur on all repeating units of COS (GlcN and GlcNAc). For all anhydrides, the equation for the degree of substitution is nearly the same, just adapted to the carbon used for the quantification. As for N-acylation, O-acylated COS with 1 equivalent of phthalic anhydride (COS-O-PA-1) could not have been characterized, due to lack of solubility in the deuterated solvents. All the ^{1}H, HSQC and quantitative ^{13}C NMR spectra of all O-acylated COS are given in supporting information (see SI, from **Figure S74** to **Figure S106**). All the resulting degrees of substitution are gathered in Table 1.

DS values are promising, as the average efficiency of the acylation is around 70 % (except for maleic anhydride whose reaction was catalyzed with pyridine). Compared to stochiometric N-acylation, the efficiency difference can be explained by the fact that hydroxyl groups are less nucleophile than amines. Furthermore, the anisyl group in COS-An undergoes steric hindrance compared to pure COS. Surprisingly, the O-acylation of COS occurred on both primary and secondary alcohols, while primary alcohols are more reactive. This observation has been made through the ^{1}H–^{13}C HSQC NMR spectrum of COS-O-SA-0.5 (see SI, **Figure S78**), where CH of glucosamine ring in the α-position of esterified secondary alcohol has been spotted at 4.4 ppm for ^{1}H and 73 ppm for ^{13}C. It is also confirmed by the quantitative ^{13}C NMR spectrum of the resulting product (Fig. 4), where the signal of CH_2 in α-position of acylated primary alcohol (62 ppm) is clearly not as intense as the signal of the reacted anhydride (30 ppm). Considering that the O-acylation without NH_2 protection did not affect secondary alcohol (see SI, **Figure S21**), it is obvious that the anisyl group used for NH_2 protection played a key role in the O-acylation. Our hypothesis is the following: the presence of the aromatic ring additionally to the imine bond that constrains the movement of the anisyl group is limiting the access of the primary alcohol, considering that the primary hydroxyl and the amine (and so the anisyl group) are both in axial positions of the cycle (whereas secondary alcohol shows equatorial position to the cycle). We believe that this interesting observation could lead to further work on the chitosan protective group and functionalization of secondary alcohols.

4. Conclusion

A simple and efficient method for selective acylation of chitooligosaccharides has been developed, and the acylation has been assessed for every compound using an innovative quantification method based on ^{13}C NMR spectroscopy. For such purpose, a preliminary model synthesis has been carried out, using glucosamine hydrochloride to represent chitosan repeating units. This model synthesis in four steps aimed at developing a strategy for the selective acylation and the ^{13}C NMR characterization.

Then, acylated COS have been synthesized using various anhydrides. Following the literature, the N-acylation has been carried out directly

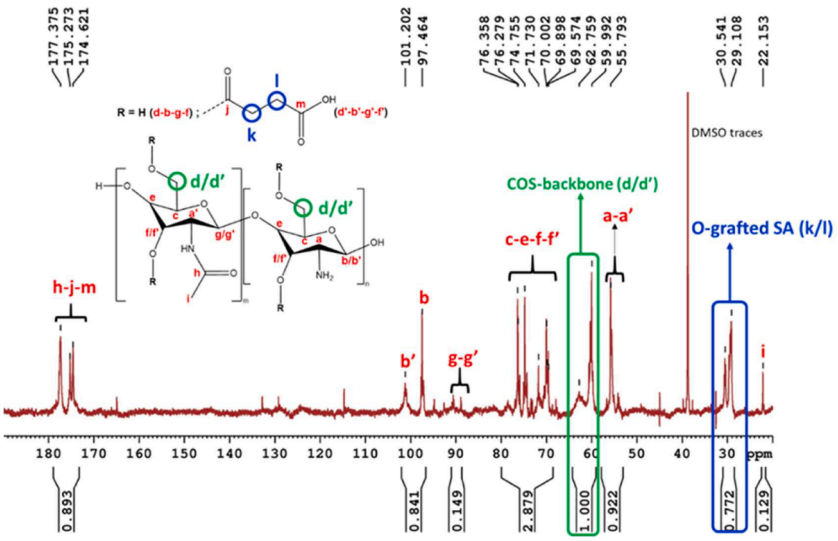

Fig. 4. ^{13}C NMR spectrum (D_2O, 125 MHz) of COS-O-SA-0.5 with the preferred signals for assessing the acylation.

with pure COS and the quantitative ^{13}C NMR analyses showed for most of the cases an experimental degree of substitution very close to the theoretical one. The resulting N-acylated COS showed no trace of O-acylation, except when no free amine groups remained.

The O-acylation of COS has been carried out in three steps, using an amine protection/deprotection method. Although anhydrides revealed to be less reactive with alcohols than with amines, the average efficiency of the O-acylation is around 70 %, which can be expected with this type of reaction. Surprisingly, the acylation occurred not only on primary alcohols but also on secondary alcohols of COS, as revealed in the HSQC spectra. The presence of anisyl group (amine protection) obviously played a key role during this step.

To conclude, the obtained results demonstrate the high reactivity of anhydrides for both amine and alcohol acylation, thus proving the potential of this chemistry to synthesize bio-based amphiphilic compounds for various applications (Aranaz et al., 2010; Chapelle et al., 2021c). Moreover, we described here the first example of quantitative ^{13}C NMR spectroscopy performed on COS. It would then be interesting to transpose and adapt these quantification methods to higher molecular weight chitosans, which could represent a step forward in the characterization of modified chitosans and derivatives.

CRediT authorship contribution statement

Paul Morandi: Writing – original draft, Visualization, Validation, Methodology, Investigation, Conceptualization. **Steve Berthalon:** Writing – original draft, Visualization, Validation, Methodology, Investigation. **Ghislain David:** Writing – review & editing, Validation, Supervision, Project administration, Funding acquisition, Conceptualization. **Aurelien Lebrun:** Writing – original draft, Visualization, Validation, Methodology, Investigation. **Karine Parra:** Writing – original draft, Visualization, Validation, Investigation. **Claire Negrell:** Writing – review & editing, Validation, Supervision, Project administration.

Declaration of competing interest

The authors declare that they have no known competing financial interests or personal relationships that could have appeared to influence the work reported in this paper.

Data availability

Data will be made available on request.

Associated content

Additional experimental details, including the amounts of reagents for the syntheses of N-acylated COS, O-acylated COS-An, O-acylated COS and the corresponding equations used to determine these amounts; NMR spectra (^{1}H, ^{13}C, HSQC and/or COSY NMR spectra) of all compounds described in this paper.

Author contributions

The manuscript was written through contributions of all authors. All authors have given approval to the final version of the manuscript.

Acknoledgements

The authors gratefully acknowledge Vietnam Food (VNF) for providing the chitooligosaccharides used in this paper.

Supplementary materials

Supplementary material associated with this article can be found, in the online version, at doi:10.1016/j.carpta.2024.100498.

References

Al-Hazmi, H. E., Łuczak, J., Habibzadeh, S., Hasanin, M. S., Mohammadi, A., Esmaeili, A., Kim, S.-J., Khodadadi Yazdi, M., Rabiee, N., Badawi, M., & Saeb, M. R. (2024). Polysaccharide nanocomposites in wastewater treatment: A review. *Chemosphere, 347*, Article 140578. https://doi.org/10.1016/j.chemosphere.2023.140578

Alvarez Echazú, M. I., Antona, M. E., Perna, O., Olivetti, C. E., Alvarez, G. S., Macri, E. V., Perez, C. J., Czerner, M., Friedman, S. M., & Desimone, M. F. (2022). Dodecenylsuccinic anhydride modified chitosan hydrogels for the sustained delivery of hydrophobic drugs. The case of thymol buccal delivery. *Journal of Applied Polymer Science, 139*, 51432. https://doi.org/10.1002/app.51432

Aranaz, I., Alcántara, A. R., Civera, M. C., Arias, C., Elorza, B., Heras Caballero, A., & Acosta, N. (2021). Chitosan: An overview of its properties and applications. *Polymers, 13*, 3256. https://doi.org/10.3390/polym13193256

Aranaz, I., Harris, R., & Heras, A. (2010). Chitosan amphiphilic derivatives. *Chemistry and Applications. COC, 14*, 308–330. https://doi.org/10.2174/138527210790231919

Bhattacharjee, M., Pramanik, N. B., Singha, N. K., & Haloi, D. J. (2020). Recent advances in RDRP-modified chitosan: A review of its synthesis, properties and applications. *Polymer Chemistry, 11*, 6718–6738. https://doi.org/10.1039/D0PY00918K

Braz, E. M. A., Silva, S. C. C. C., Sousa Brito, C. A. R., Brito, L. M., Barreto, H. M., Carvalho, F. A. A., Santos, L. S., Lobo, A. O., Osajima, J. A., Sousa, K. S., & Silva-Filho, E. C. (2020). Spectroscopic, thermal characterizations and bacteria inhibition of chemically modified chitosan with phthalic anhydride. *Materials Chemistry and Physics, 240*, Article 122053. https://doi.org/10.1016/j.matchemphys.2019.122053

Chapelle, C., David, G., Caillol, S., Negrell, C., Catrouillet, S., Le Foll, M. D., & Azéma, N. (2021a). Surfactant properties of chemically modified chitooligosaccharides and their potential application in bitumen emulsions. *Colloids and Surfaces A: Physicochemical and Engineering Aspects, 628*, Article 127327. https://doi.org/10.1016/j.colsurfa.2021.127327

Chapelle, C., David, G., Caillol, S., Negrell, C., & Desroches Le Foll, M. (2021b). Advances in chitooligosaccharides chemical modifications. *Biopolymers, 112*. https://doi.org/10.1002/bip.23461

Chapelle, C., David, G., Caillol, S., Negrell, C., Durand, G., & le Foll, M. D. (2021c). Functionalization of chitosan oligomers: From aliphatic epoxide to cardanol-grafted oligomers for oil-in-water emulsions. *Biomacromolecules, 22*, 846–854. https://doi.org/10.1021/acs.biomac.0c01576

Chotphruethipong, L., Chanvorachote, P., Reudhabibadh, R., Singh, A., Benjakul, S., Roytrakul, S., & Hutamekalin, P. (2023). Chitooligosaccharide from pacific white shrimp shell chitosan ameliorates inflammation and oxidative stress via NF-κB, Erk1/2, Akt and Nrf2/HO-1 pathways in LPS-induced RAW264.7 macrophage cells. *Foods (Basel, Switzerland), 12*, 2740. https://doi.org/10.3390/foods12142740

Cunha, A. C., Pereira, L. O. R., de Souza, M. C. B. V., & Ferreira, V. F. (1999). Use of protecting groups in carbohydrate chemistry: an advanced organic synthesis experiment. *J. Chem. Educ., 76*, 79. https://doi.org/10.1021/ed076p79

Don, T.-M., & Chen, H.-R. (2005). Synthesis and characterization of AB-crosslinked graft copolymers based on maleilated chitosan and N-isopropylacrylamide. *Carbohydrate Polymers, 61*, 334–347. https://doi.org/10.1016/j.carbpol.2005.05.025

Fu, Y., He, H., Liu, R., Zhu, L., Xia, Y., & Qiu, J. (2019). Preparation and performance of a BTDA-modified polyurea microcapsule for encapsulating avermectin. *Colloids and Surfaces B: Biointerfaces, 183*, Article 110400. https://doi.org/10.1016/j.colsurfb.2019.110400

Gopal Reddi, M. R., Gomathi, T., Saranya, M., & Sudha, P. N. (2017). Adsorption and kinetic studies on the removal of chromium and copper onto Chitosan-g-maliec anhydride-g-ethylene dimethacrylate. *International Journal of Biological Macromolecules, 104*, 1578–1585. https://doi.org/10.1016/j.ijbiomac.2017.01.142

Hasipoglu, H. N., Yilmaz, E., Yilmaz, O., & Caner, H. (2005). Preparation and characterization of maleic acid grafted chitosan. *International Journal of Polymer Analysis and Characterization, 10*, 313–327. https://doi.org/10.1080/10236660500479478

Holmes, E. B., Oza, H. H., Bailey, E. S., & Sobsey, M. D. (2023). Evaluation of Chitosans as Coagulants—Flocculants to improve sand filtration for drinking water treatment. *IJMS, 24*, 1295. https://doi.org/10.3390/ijms24021295

Ifuku, S., Miwa, T., Morimoto, M., & Saimoto, H. (2011). Preparation of highly chemoselective N-phthaloyl chitosan in aqueous media. *Green Chemistry : An International Journal and Green Chemistry Resource : GC, 13*, 1499. https://doi.org/10.1039/c0gc00860e

Kou, S.(G.), Peters, L., & Mucalo, M. (2022). Chitosan: A review of molecular structure, bioactivities and interactions with the human body and micro-organisms. *Carbohydrate Polymers, 282*, Article 119132. https://doi.org/10.1016/j.carbpol.2022.119132

Madera-Santana, T. J., Herrera-Méndez, C. H., & Rodríguez-Núñez, J. R. (2018). An overview of the chemical modifications of chitosan and their advantages. *Green Materials, 6*, 131–142. https://doi.org/10.1680/jgrma.18.00053

Mayahi, M. F., & El-Bermani, M. F. (1973). Maleic anhydride – triethylamine complex. *Candian Journal of Chemistry, 51*, 3539–3540. https://doi.org/10.1139/v73-527

Meyer-Déru, L., David, G., & Auvergne, R. (2022). Chitosan chemistry review for living organisms encapsulation. *Carbohydrate Polymers, 295*, Article 119877. https://doi.org/10.1016/j.carbpol.2022.119877

Mohammad El-Aidie, S. A.-A. (2018). A review on chitosan: Ecofriendly multiple potential applications in the food industry. *IJALSR, 1*, 1–14. https://doi.org/10.31632/ijalsr.2018v01i01.001

Morin-Crini, N., Lichtfouse, E., Torri, G., & Crini, G. (2019). Applications of chitosan in food, pharmaceuticals, medicine, cosmetics, agriculture, textiles, pulp and paper, biotechnology, and environmental chemistry. *Environmental Chemistry Letters, 17*, 1667–1692. https://doi.org/10.1007/s10311-019-00904-x

Mourya, V. K., Inamdar, N. N., & Choudhari, Y. M. (2011). Chitooligosaccharides: Synthesis, characterization and applications. *Polymer Science Series A, 53*, 583–612. https://doi.org/10.1134/S0965545X11070066

Naveed, M., Phil, L., Sohail, M., Hasnat, M., Baig, M. M. F. A., Ihsan, A. U., Shumzaid, M., Kakar, M. U., Mehmood Khan, T., Akabar, Md., Hussain, M. I., & Zhou, Q.-G. (2019). Chitosan oligosaccharide (COS): An overview. *International Journal of Biological Macromolecules, 129*, 827–843. https://doi.org/10.1016/j.ijbiomac.2019.01.192

Nasrollahzadeh, M., Shafiei, N., Nezafat, Z., Soheili Bidgoli, N. S., & Soleimani, F. (2020). Recent progresses in the application of cellulose, starch, alginate, gum, pectin, chitin and chitosan based (nano)catalysts in sustainable and selective oxidation reactions: A review. *Carbohydrate Polymers, 241*, Article 116353. https://doi.org/10.1016/j.carbpol.2020.116353

Nguyen, T. N., Huynh, T. N., Hoang, D., Nguyen, D. H., Nguyen, Q. H., & Tran, T. H. (2019). Functional nanostructured oligochitosan–silica/carboxymethyl cellulose hybrid materials: Synthesis and investigation of their antifungal abilities. *Polymers, 11*, 628. https://doi.org/10.3390/polym11040628

Ranjbar-Mohammadi, M., Arami, M., Bahrami, H., Mazaheri, F., & Mahmoodi, N. M. (2010). Grafting of chitosan as a biopolymer onto wool fabric using anhydride bridge and its antibacterial property. *Colloids and Surfaces B: Biointerfaces, 76*, 397–403. https://doi.org/10.1016/j.colsurfb.2009.11.014

Shetgiri, N. P., & Nayak, B. K. (2005). Synthesis and antimicrobial activity of some succinimides. *Indian Journal of Chemistry*.

Shrestha, R., Thenissery, A., Khupse, R., & Rajashekara, G. (2023). Strategies for the preparation of chitosan derivatives for antimicrobial, drug delivery, and agricultural applications: A review. *Molecules (Basel, Switzerland), 28*, 7659. https://doi.org/10.3390/molecules28227659

Sousa, J. M., Vieira, A. C. C., Costa, M. P., Rizzo, M. S., Chaves, L. L., Braz, E. M. A., Bezerra, R. D. S., Leal, R. C., Barreto, H. M., Osajima, J. A., & Silva-Filho, E. C. (2022). Chitosan grafted with maleic anhydride and ethylenediamine: Preparation, characterization, computational study, antibacterial and cytotoxic properties. *Materials Chemistry and Physics, 287*, Article 126301. https://doi.org/10.1016/j.matchemphys.2022.126301

Vårum, K. M., Antohonsen, M. W., Grasdalen, H., & Smidsrød, O. (1991). Determination of the degree of N-acetylation and the distribution of N-acetyl groups in partially N-deacetylated chitins (chitosans) by high-field N.M.R. spectroscopy. *Carbohydrate Research, 211*, 17–23. https://doi.org/10.1016/0008-6215(91)84142-2

Yang, R., Li, H., Huang, M., Yang, H., & Li, A. (2016). A review on chitosan-based flocculants and their applications in water treatment. *Water Research, 95*, 59–89. https://doi.org/10.1016/j.watres.2016.02.068

Yao, H.-Y.-Y., Wang, J.-Q., Yin, J.-Y., Nie, S.-P., & Xie, M.-Y. (2021). A review of NMR analysis in polysaccharide structure and conformation: Progress, challenge and perspective. *Food Research International, 143*, Article 110290. https://doi.org/10.1016/j.foodres.2021.110290

Zhang, W., Li, G., Fang, Y., & Wang, X. (2007). Maleic anhydride surface-modification of crosslinked chitosan membrane and its pervaporation performance. *Journal of Membrane Science, 295*, 130–138. https://doi.org/10.1016/j.memsci.2007.03.001

Zhang, X., Ding, C., Liu, H., Liu, L., & Zhao, C. (2011). Protective effects of ion-imprinted chitooligosaccharides as uranium-specific chelating agents against the cytotoxicity of depleted uranium in human kidney cells. *Toxicology, 286*, 75–84. https://doi.org/10.1016/j.tox.2011.05.011